

Modeling and Simulation of Flue Gas Desulfurization Using Slurry of Fine Activated Carbon Particles

Dr. Neran K. Ibrahim* & Asmaa I. Eliass*

Received on: 28/12/2009

Accepted on: 1 1/3/2010

Abstract

The main objective of the present work is to investigate the feasibility of using a slurry of fine activated carbon particles, $d_p < 1\text{mm}$, in a fixed bed reactor for the removal of sulfur dioxide from simulated flue gas (air, SO_2) stream. A mathematical model governing the desulfurization process was proposed. The partial differential equations which describe the adsorption of SO_2 from a moving gas stream to the sorbent bed were solved using a finite difference method. The kinetic parameters of the mathematical model were obtained from a series of experimental desulfurization runs carried out at isothermal conditions and different operating conditions; bed temperature (333K-373K), initial SO_2 concentration (500ppm-2000ppm) and static bed height (10cm-24cm). The results showed that the use of fine activated carbon particles improved the removal efficiency to about 97%. The verification of the simulation and experimental results showed that the proposed model gave a good description of the desulfurization process with 95% confidence level.

Keywords: Desulfurization, Slurry reactor, Activated carbon, Modeling; Simulation; Finite difference

النموذج المحاكائي لعملية إزالة الكبريت من الغاز العادم باستخدام مفاعل ثلاثي الأطوار

الخلاصة

يتضمن البحث دراسة جدوى استخدام الفحم المنشط الرطب ذواقطاردقائلا لتتعدى ال 1 ملم في مفاعل ذو حشوة ثابتة لازالة غاز ثنائي اوكسيد الكبريت من مجرى غازي محاكي لمجرى الغازات العادمة (هواء , SO_2). تم اقتراح موديل رياضي يصف عملية الازالة المعادلات التفاضلية الجزئية والتي تصف عملية امتزاز ال SO_2 من مجرى غازي الى سطح المادة الممتزة تم حلها باستخدام طريقة الفروق المحددة. المعاملات الحركية للموديل الرياضي تم استخراجها من سلسلة من التجارب اجريت في درجات حرارة ثابتة. وظروف عمل مختلفة: حرارة المفاعل (333-373 كلفن), التركيز البدائي لل SO_2 (500-2000 جزء من المليون) وارتفاع الحشوة (10-24 سم). النتائج اظهرت ان استخدام دقائلا الكاربون المنشط ذات الاقطار الصغيرة لت الى زيادة كفاءة الازالة ال SO_2 الى ما يقارب ال 97%. عند مقارنة نتائج الموديل الرياضي الذي تم اقتراحه مع النتائج العملية اظهرت المقارنة ان الموديل المقترح اعطى تفسيراً جيداً لعملية الازالة ال SO_2 و بدرجة ثقة 95%.

1-Introduction

Environmental regulations all over the world are becoming more restrictive concerning the release of atmospheric pollutants associated with the flue gases of combustion systems, particularly the emission of sulphur dioxide SO_2 . The concentration of SO_2 in the flue gas produced by combustion facilities ranges from 500 to 2000 ppm, whereas most environmental regulations throughout the world only permit about 50 to 100 ppm. Therefore, flue gas from the power plant has to be treated with appropriate yet affordable desulfurization technology before it can be emitted to the environment.

Cho (1986) reported that activated carbon which contains the catalysis of ferric/ferrous ions for the reaction between SO_2 and O_2 has been known for many years. The oxidation reactions occur by three routes. First, SO_2 particles diameter of activated carbon.

Gao *et al.* (2001) studied desulfurization process in a coke activation reactor of FGD system. The effect of flue gas temperature, particle size, water addition and coke molar ratio on desulfurization efficiency was investigated. It was found that desulfurization efficiency rises with the increase of coke molar ratio, the amount of water addition, flue gas temperature and decrease of particle size.

serves as a reducing reagent of ferric ion. Second, SO_2 together with O_2 serves as an oxidizing reagent of ferrous ion to ferric ion. Third, ferric ion catalyzes the oxidation reaction of SO_2 .

Lizzio and DeBarr (1997) showed that the reaction of SO_2 with carbon in the presence of O_2 (in air) and H_2O involves a series of reactions that leads to the formation of sulfuric acid as the final product. The rate-determining step in the overall process is the oxidation of SO_2 to SO_3 .

Liu and Kato (2000) used a semidry method for the removal of SO_2 from simulated flue gas stream. The removal was achieved by using powder-particle slurry bed of activated carbon. It was found that the SO_2 removal efficiency increases with the increase of temperature, relative humidity and height of bed and decreases with the increase of initial concentration of SO_2 and

Bagreev *et al.* (2001) showed that the normalized capacity of the activated carbon adsorbents, especially at higher temperature is much larger than that of the activated carbon at lower temperature.

Cho and Miller (2002) studied the overall removal efficiency of sulfur dioxide from flue gas with coal scrubbing; the objective of the study was to determine the effects of temperature, oxygen concentration and SO_2 concentration on SO_2 removal

from simulated flue gas streams and on leaching rate of coal pyrite.

Bagreev and Bandosz (2003) showed for the removal of SO₂ using coal slurry the importance of the role of water in the formation of sulfuric acid in pore system.

Recently, Jawad (2007) studied the effect of temperature, SO₂ initial concentration and flue gas flow rate on the overall removal efficiency of SO₂ using a slurry of activated carbon with particles of a mean diameter, dp > 1.0 mm. The results showed that the removal efficiency increases with increasing bed temperature and decreasing SO₂ initial concentration. An optimum value of 60 l/min for the flue gas flow rate was obtained.

In the present study, and in order to investigate the effect of particle size and bed height on the removal efficiency of SO₂, a series of experimental desulfurization tests were conducted using slurry of activated carbon particles, with mean particle diameter, dp_m < 1mm. The effect of the operating variables on the overall removal efficiency of SO₂ was examined and the results were compared with a proposed mathematical model based on the mass balance for gaseous and solid phases.

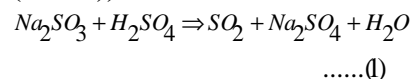
3- Experimental Work

The experiments were carried out in a laboratory scale apparatus which is shown

schematically in Figure (1). The test section consists of a cylindrical column of (7.5) cm inside diameter and (50) cm height filled to the required bed height with a slurry of fine activated carbon particles (dp_m=0.70 mm). An external heater of 224watt, wrapped around the reactor, was used to heat the bed to the required temperature. The chemical analysis and the physical properties of the activated carbon used in this study were given in tables (1 and 2), respectively.

Experimental Procedure

A slurry of activated carbon was prepared by immersing the required quantity of activated carbon bed with (1/2) liter of water in the reactor. Sulfur Dioxide gas was synthesized by dropping the desired concentration of sulfuric acid into the SO₂ generation flask that contains the aqueous sodium sulfite solution according to the following chemical reaction (Lippert et al. (1994)):



After adjusting the bed temperature to the desired value, the air stream at an optimum value of 20 l/min (Eliass (2008)) was passed through the generation flask to carry the SO₂ to the test section. In order to measure the concentration of SO₂ in the effluent gas stream, (10) ml of

the iodine sample was taken from the absorption trap, titrated with standard sodium thiosulphate solution (0.1 N, in the presence of starch indicator. This step was repeated every 5 minutes till the end of experimental run time (1 hr). The removal efficiency of SO₂ was calculated as the ratio of SO₂ concentration that was adsorbed by activated carbon to the initial concentration of SO₂ gas fed to the bed.

$$h (\%) = \frac{C_0 - C_{so_2}}{C_0} * 100 \quad \dots(2)$$

4-Model Development

The following assumptions were used to formulate the mathematical model: constant porosity, spherical solid particle, dispersion radial and axial directions are neglected (i.e. plug flow), and isothermal process.

- For the Gas Phase

$$F_{so_2} \Big|_{z+\Delta z} - F_{so_2} \Big|_{z-\Delta z} - r_{so_2} (A_R \Delta z) = e r (A_R \Delta z) \frac{\partial C_{so_2}}{\partial t} \quad (3)$$

$$\frac{n}{L A_R} \frac{\partial Y}{\partial Z} + e r C_0 \frac{\partial Y}{\partial t} + \frac{S_e w}{V_R} r_{so_2} = 0 \quad \dots(4)$$

- For the Solid Phase:-

$$-(-r_{so_2}) v_s S_e M = \frac{\partial (C_o - C_{so_2})}{\partial t} \quad \dots(5)$$

$$\frac{(C_o - C_{so_2})}{C_o} = X \quad \dots(6)$$

Sorbent Conversion

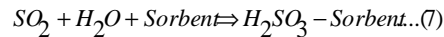
Rearranging equation 5 gives :

$$\frac{\partial X}{\partial t} = r_{so_2} v_s S_e M \quad \dots(7)$$

To solve equations (4) and (6) the following initial boundary conditions were used:

- a - at t = 0 & Z > 0 ⇒ Y = 0, X = 0
- b - at Z = 0 & t > 0 ⇒ Y = 1

In order to solve the differential equations (4) and (6), a rate expression of the desulfurization reaction, SO₂ was assumed to react with water molecules in the presence of the sorbent to form H₂SO₃ according to the reaction:



The rate of reaction (r_{so2}) for the desulfurization reaction over the sorbent can be expressed as a product of a temperature dependent rate constant k(T) and the concentration of the reactants (Fogler (1983)) .

$$r_{so_2} = \frac{dX}{dt} = k(T) [SO_2]^\alpha [H_2O]^\beta \dots(8)$$

Where (α) is the order of the reaction with respect to SO₂ and (β) is the order of the reaction with respect to H₂O. Assuming that the concentration of H₂O is in excess as compared to SO₂, Eq. (8) can be simplified to:

$$\frac{dX}{dt} = k(T) C_o (1-X)^a (RH)^b \quad \dots(9)$$

Where (C_o) is the initial concentration of SO₂ and (RH) is the relative humidity of the feed gas.

The temperature dependent rate constant in Eq. (9) is taken as the global reaction rate constant which obeys the Arrhenius Law (Smith (2000)), k, given by:

$$k(T) = k = A_f \exp\left(-\frac{E}{RT}\right) \dots (10)$$

Where (E) is the activation energy of the desulfurization reaction, (A_f) is the frequency or pre-exponential factor of the desulfurization reaction and (R) is the universal gas constant. The rate expression for the desulfurization reaction can be written as:

$$r_{so_2} = A_f \exp\left(-\frac{E}{RT}\right) C_o (1-X)^a (RH)^b \dots(11)$$

With the inclusion of effectiveness factor (ξ) in the rate expression, it is written as:

$$r_{so_2} = \alpha A_f \exp\left(-\frac{E}{RT}\right) C_o (1-X)^a (RH)^b \quad \dots(12)$$

The effectiveness factor is taken as a constant equal to 0.9. In order to obtain the values of (A_f, α, E and β) Eq. (12) was substituted into Eq. (4) and Eq. (6), yielding Eqs.(13) and Eq. (14).

For the gas phase:-

$$\frac{n}{L A_R} \frac{\partial Y}{\partial Z} + e r C_o \frac{\partial Y}{\partial t} + \frac{S_e w}{V_R} \left[\alpha A_f \exp\left(-\frac{E}{RT}\right) C_o (1-X)^a (RH)^b \right] = 0$$

For the solid phase:-

$$\frac{\partial X}{\partial t} = v_s S_e M \left[\alpha A_f \exp\left(-\frac{E}{RT}\right) C_o (1-X)^a (RH)^b \right] \dots (14)$$

From Eq.(13) :

$$e r C_o \frac{\partial Y}{\partial t} = \frac{n}{L A_R} \frac{\partial Y}{\partial Z} + \frac{S_e w}{V_R} \left[\alpha A_f \exp\left(-\frac{E}{RT}\right) C_o (1-X)^a (RH)^b \right] \dots(15)$$

$$\frac{\partial Y}{\partial t} = -\frac{1}{e r C_o} \frac{n}{L A_R} \frac{\partial Y}{\partial Z} - \frac{1}{e r C_o} \frac{S_e w}{V_R} \left[\alpha A_f \exp\left(-\frac{E}{RT}\right) C_o (1-X)^a (RH)^b \right] \quad (16)$$

$$\frac{Y_{(i)}^{N+1} - Y_{(i)}^N}{\Delta t} = -\frac{1}{e r C_o} \frac{n}{L A_R} \frac{Y_{(i+1)}^N - Y_{(i-1)}^N}{2^* \Delta Z} - \frac{1}{e r C_o} \frac{S_e w}{V_R} \left[\alpha A_f \exp\left(-\frac{E}{RT}\right) C_o (1-X)^a (RH)^b \right] \dots (17)$$

$$Y_{(i)}^{N+1} = Y_{(i)}^N - \frac{\Delta t}{e r C_o} \frac{n}{L A_R} \frac{Y_{(i+1)}^N - Y_{(i-1)}^N}{2^* \Delta Z} - \frac{\Delta t}{e r C_o} \frac{S_e w}{V_R} \left[\alpha A_f \exp\left(-\frac{E}{RT}\right) C_o (1-X)^a (RH)^b \right] \dots(18)$$

The ordinary differential equation was solved numerically. The values of (A_f, α, E and β) were then obtained by least-square fitting of the solved ordinary differential equation to the experimental data. A computer program has been developed in Fortran N90 to perform the numerical solution formulated previously.

The values of A_p , α , E and β were found to be 1.07, 2.2, 22.9 kJ/mol and 3.1 respectively.

5- Results & Discussion

Figures (2 to 4) show the effect of temperature on the overall removal efficiency of SO_2 for different initial SO_2 concentrations in flue gas stream, and different bed heights. The trends of the results indicate that SO_2 removal was temperature sensitive, giving overall removal of 85% at 30 °C and 89% at 80 °C after 24 hours. The results also indicate that for constant bed temperature and constant bed height, the overall removal efficiency decreases as the initial concentration of SO_2 in the simulated gas increases. The decrease in the bed activity is a direct consequence of exposing a fixed amount of the sorbent to the increasing concentration of SO_2 .

Figure (5) shows the direct effect of activated carbon particle diameter on the overall removal efficiency of SO_2 for wet and dry bed conditions. The results show a higher value for the removal efficiency of 97% for $d_p=0.7$ mm as compared to around 94% for $d_p=1.5$ mm. The data for particle size of $d_p=1.5$ mm was obtained from a previous study (Jawad (2007)) conducted under similar operating conditions. For similar experimental conditions, while the sorbent particle diameter is smaller, the chemical reaction

area is greater because there are more sorbent particles in the bed. Moreover, the increases in particle diameter imply that the SO_2 diffusion path in particles rises and the result of uniform humidification becomes worse because increasing the particle size results in the decrease of contact area among gas, liquid and solid three phases, which is unfavorable to reaction. The figure also shows the importance of the role of water on the adsorption mechanism. The SO_2 removal is higher in wet beds as compared to dry beds; this is mainly due to the increase in chemical reaction rate.

Figure (6) shows the change of the SO_2 removal efficiency with time for different static bed heights at $C_0=2000$ ppm, $T=80$ °C. The results show an increase in the overall removal efficiency of SO_2 by about 1% when the bed height increased by 14 cm. This is mainly due to the increase in the contact time between the polluted gas and the sorbent. Also more active sites will be available as the bed height increased.

Figures (7&8) show a comparison between the simulation and experimental results for two different bed temperatures. These Figures clarify that the model gives a very good predications for the experimental data. However, in these figures the deviation is probably due to the agglomeration of some sorbent

particles because of their great cohesive force, and the effective chemical reaction area between the flue gas and the sorbent particles is therefore reduced.

Figure (9) shows the axial distribution of SO_2 concentration along the bed height at different operating times. The results indicate that the proposed model succeeded in representing the experimental data with 95% confidence level using the goodness of fit test (Subhi (1990)).

The breakthrough curves of the sorbent for different static bed heights are shown in figure (10).

6-Conclusions

From the above study the following conclusions may be drawn; the SO_2 removal efficiency increases with increasing bed temperature, height, humidity and decreasing sorbent diameter. A reduction in the SO_2 removal efficiency was observed with increasing SO_2 initial concentration in the flue gas stream. The mathematical model proposed was found to provide a good description of the desulfurization reaction under conditions prevailing in the flue gas desulfurization process at higher temperature.

References

[1] Bagreev, A., and Bandosz, T. J., 2003. "Carbon", Department of Chemical

Engineering, University of New York.

[2] Bagreev, A., Bashkova, S., Locke, D. C., and Bandosz, T. J., 2001. "Sewage sludge-derived materials as adsorbents of SO_2 ", Department of Chemical Engineering, University of New York.

[3] Cho, E. H., 1986. "Removal of SO_2 with oxygen in the presence of Fe (III)", *Met.Trans.B*, Vol. 17B, PP. (745-753).

[4] Cho, E. H., and Miller, H. L., 2002. "SO₂ removal with coal scrubbing", M.Sc. thesis, University of West Virginia.

[5] Eliass, A. I., 2008. "Experimental and simulation study of flue gas desulfurization using slurry reactor", M.Sc. thesis, University of Technology, Baghdad, Iraq.

[6] Fogler, H. S., 2005. "Elements of chemical reaction engineering", 4th Ed., Prentice-Hall.

[7] Ao, X., Luo, Z. Liu, N., Ni, M., and Can, K., 2001. "Desulfurization characteristic of carbon-based sorbent during activation process", *Zhejiang University, J. of Chem. Eng. Of Japan*, Vol. 34, No. 9, PP. (1114-1119).

[8] Jawad, Z., A., 2007. "Sulfur dioxide removal in coal slurry reactor", M.Sc. thesis, University of Technology, Baghdad, Iraq.

[9] Lippert, B., P., Stejskalora, K., and Mocek, K., 1994. *Chemike Listy*, Vol.88, PP. (60-61).

[10] Liu, Y., and Kato, K., 2000. "Process analysis of semidry desulfurization process in powder particle spouted bed", Department of Biological and Chemical Engineering, Gunma University, J. of Chem. Eng., Vol 33, No.2, PP. (223-231).

[11] Lizzio, A., A., and DeBarr, J., A., 1997. "Mechanism of SO₂ removal by carbon", Department of Environmental Engineering and Science, University of Illinois.

[12] Smith, J. M., and Van Ness, H. C., 2000. "Introduction to chemical engineering thermodynamics", 4th Ed., Inc. New York, PP. (300).

[13] Subhi, M., and Awad, A., 1990. "Introduction to statistics", 1st Ed., Jordanian Book Center, Amman.

Nomenclature:

A_R transversal bed section, m²
 a specific area of the bed m²/m³
 A_f frequency factor or pre-exponential factor, s⁻¹
 T temperature, °C
 t time, s or min
 u axial superficial velocity of gas, m.s⁻¹
 vs stoichiometric coefficient, [-]
 V_{STP} volume of gas at standard temperature and pressure, l
 ξ effectiveness factor, [-]
 ρ molar density of solid particles, mole.m⁻³

C_0 initial concentration of sulfur dioxide, ppm
 C_{SO_2} effluent concentration of sulfur dioxide, ppm
 C sulfur Dioxide concentration ppm
 dp slurry particle diameter, mm
 E activation energy, kJ.mol⁻¹
 F molar rate, mole/s
 k global reaction rate constant, s⁻¹
 $k(T)$ temperature dependent rate constant, s⁻¹
 L bed length, m
 M molecular weight of activated carbon, g.mol⁻¹
 n molar flow rate of SO₂, mol.s⁻¹
 N time interval, [-]
 Q flow rate of SO₂, l/min
 R universal gas constant, J.mol⁻¹.K⁻¹
 RH relative humidity, [%]
 r_{SO_2} reaction rate, mol.m⁻².s⁻¹
 Se specific surface area, m².g⁻¹
 V_R volume of the reaction bed, m³
 w sorbent weight in the bed, g
 X sorbent conversion, [-]
 Y dimensionless SO₂ concentration, (C/C₀) [-]
 Z dimensionless length position, [-]
 ϵ bed porosity, [-]

Table (1) Chemical analysis of activated carbon

Material	wt %	Material	wt%
C	92.46	Mg⁺²	3.250
Ca⁺²	2.750	Mn⁺²	0.116
Co⁺²	0.075	Pb⁺²	0.513
Cu⁺²	0.150	PO₄⁻⁴	0.018
Fe⁺²	0.070	SO₄⁻²	0.018
Fe⁺³	0.325	Zn⁺²	0.025

Table (2) Physical properties of activated carbon

Surface area	1122.13 (m² / g)
Bulk density	0.4423 (g /cm³)
Porosity	0.48972 (-)

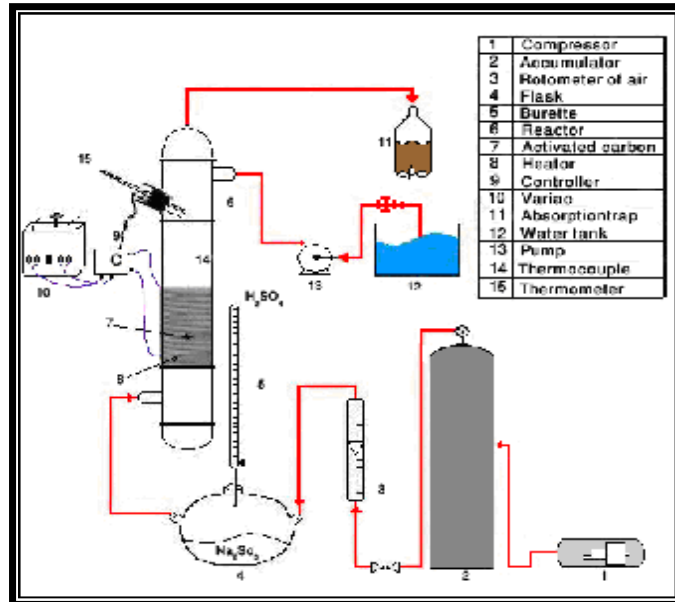


Figure (1) Schematic Diagram of the Experimental Setup

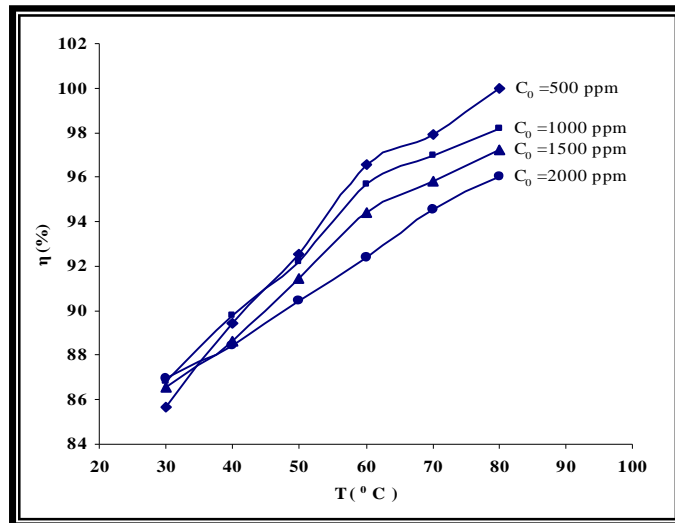


Figure (2) The effect of bed temperature on the overall removal efficiency of SO₂ for different initial SO₂ concentration and bed height of 10 cm

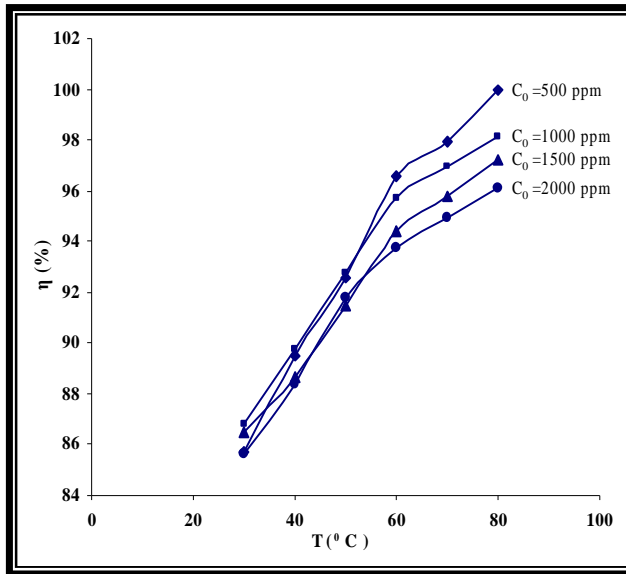


Figure (3) The effect of bed temperature on the overall removal efficiency of sulfur dioxide for different initial SO₂ concentration and bed height of 18 cm

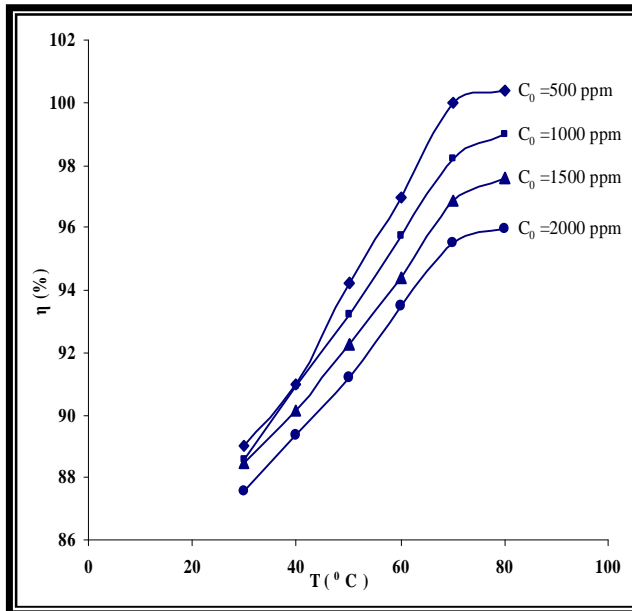


Figure (4) The effect of bed temperature on the overall removal efficiency of SO₂ for different initial SO₂ concentration and bed height of 24 cm

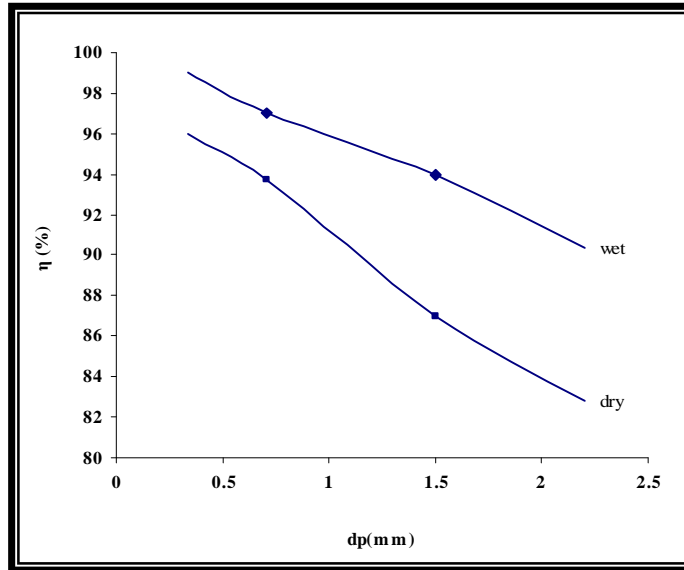


Figure (5) The effect of particle diameter on the overall removal efficiency of SO_2 , $C_0=2000$ ppm,

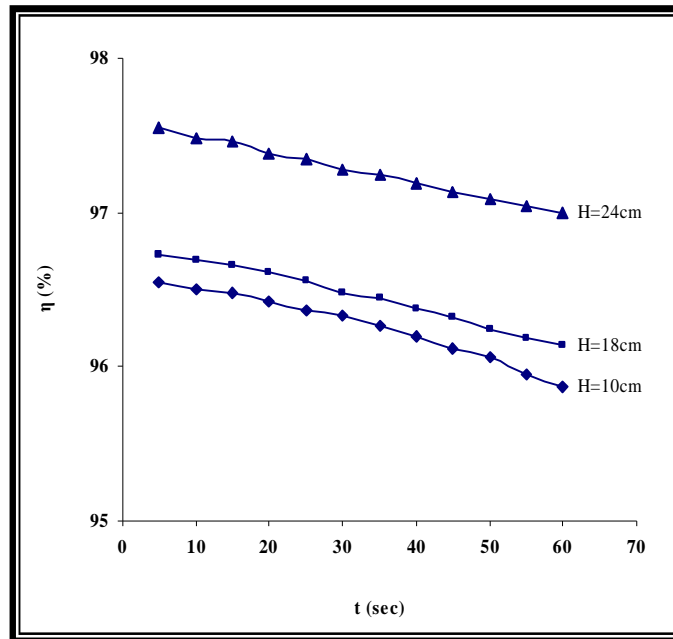


Figure (6) The change of the overall SO_2 removal efficiency with time for different bed heights at $C_0=2000$ ppm and $T=80^\circ\text{C}$

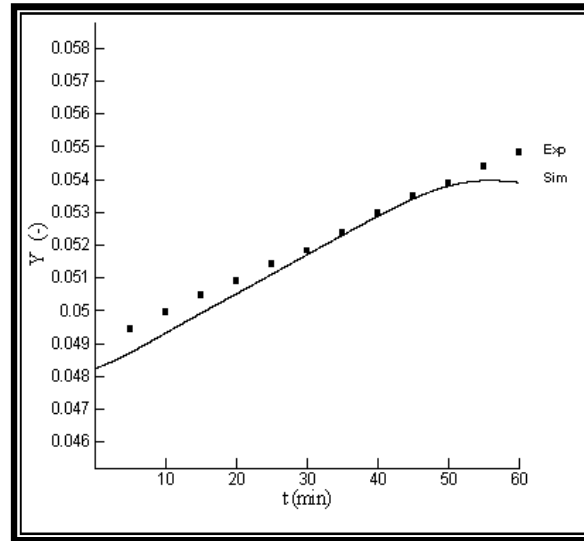


Figure (7) Comparison between simulation and experimental results at $C_0=2000$ ppm and $T=70$ °C

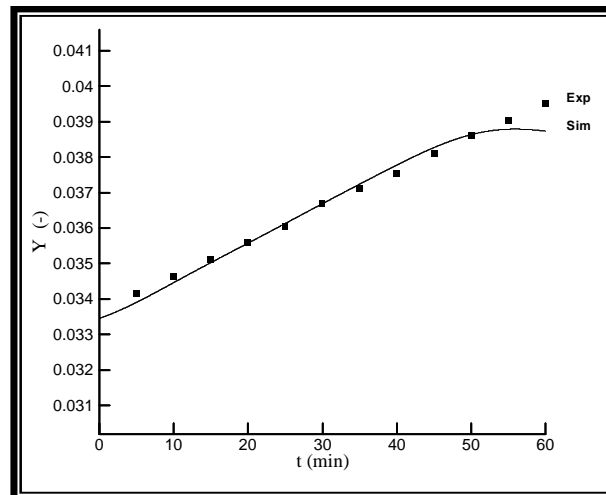


Figure (8) Comparison between simulation and experimental results at $C_0=2000$ ppm and $T=80$ °C

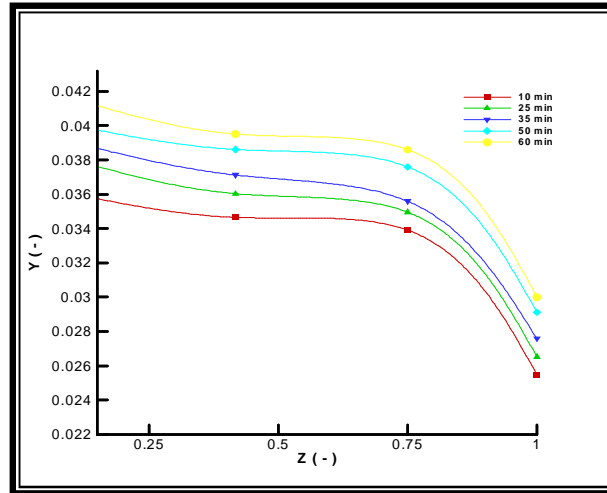


Figure (9) The axial distribution of SO₂ concentration along the bed height for C₀=2000 ppm and T=80 °C

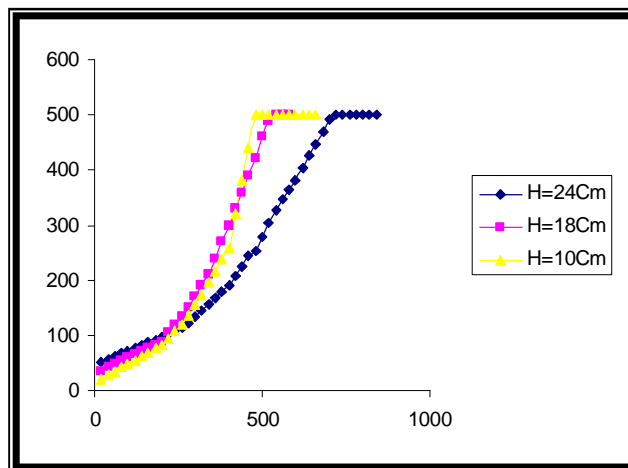


Figure (10) The breakthrough life of activated carbon for different bed heights at C₀=500 ppm and T=80 °C